AGU PUBLICATIONS

Geophysical Research Letters

RESEARCH LETTER
10.1002/2017GL074110

Key Points:
- We compute the fracture energy associated with flash heating in an updated model accounting for bulk thermal effects
- Flash heating explains laboratory friction data obtained under imposed slip rate conditions
- The fracture energy for flash heating during earthquakes is small compared to thermal pressurization and off-fault energy dissipation

Supporting Information:
- Supporting Information S1

Correspondence to:
N. Brantut,
n.brantut@ucl.ac.uk

Citation:
Brantut, N., and R. C. Viesca (2017), The fracture energy of ruptures driven by flash heating, *Geophys. Res. Lett.*, *44*, doi:10.1002/2017GL074110.

Received 10 MAY 2017
Accepted 26 JUN 2017
Accepted article online 5 JUL 2017

The fracture energy of ruptures driven by flash heating

Nicolas Brantut[1] **and Robert C. Viesca**[2]

[1]Rock and Ice Physics and Seismological Laboratory, Department of Earth Sciences, University College London, London, UK, [2]Department of Civil and Environmental Engineering, Tufts University, Medford, Massachusetts, USA

Abstract We present a model for dynamic weakening of faults based on local flash heating at microscopic asperity contacts coupled to bulk heating at macroscopic scale. We estimate the fracture energy G associated with that rheology and find that for constant slip rate histories G scales with slip δ as $G \propto \delta^2$ at small slip, while $G \propto \delta^{1/2}$ at large slip. This prediction is quantitatively consistent with data from laboratory experiments conducted on dry rocks at constant slip rate. We also estimate G for crack-like ruptures propagating at constant speed and find that $G \propto \delta^{2/3}$ in the large slip limit. Quantitative estimates of G in that regime tend to be several orders of magnitude lower than seismologically inferred values of G. We conclude that while flash heating provides a consistent explanation for the observed dynamic weakening in laboratory experiments with kinematically imposed slip, its contribution to the energy dissipation during earthquakes becomes negligible for large events when considering the elastodynamic coupling between strength and slip evolution.

1. Introduction

The dynamics of earthquakes is primarily controlled by the balance between the available elastic strain energy (i.e., the prerupture stress level along the fault), the energy radiated away from the fault, and the fracture energy G consumed to advance the rupture front. The fracture energy, far from being a material constant, depends on how the fault weakens during slip and hence is ultimately controlled by the physical processes responsible for fault weakening.

In the context of seismology and shear rupture propagation with complex friction laws, G is generally defined by the integral of the shear strength change over the local slip [e.g., *Kanamori and Heaton*, 2000; *Abercrombie and Rice*, 2005]. Therefore, G integrates potentially complex strength evolution with slip, slip rate, and other evolving physical variables. Far-field seismological observations provide constraints on the magnitude of G, which is typically derived from estimates of moment magnitude, stress drop, and radiated energy [e.g., *Abercrombie and Rice*, 2005; *Viesca and Garagash*, 2015]. However, disentangling the details of stress, slip or slip rate evolution from G, is generally not possible (or at least not unequivocally) with seismological data alone [e.g., *Guatteri and Spudich*, 2000]. Hence, the physical mechanisms giving rise to earthquake propagation remain only accessible through a single integrated quantity, the fracture energy.

One approach to circumvent this issue and identify the underlying physics of dynamic weakening is to make predictions of G based either on empirical laboratory data [*Nielsen et al.*, 2016] or theoretical analysis [*Rice*, 2006; *Viesca and Garagash*, 2015] and examine if and how the resulting scaling of G with other source parameters (typically, fault slip) matches with independent seismological estimates. In other words, the key question is: what does the observed scaling of G tell us about the physics of rupture? Such an approach has been remarkably successful in identifying thermal pressurization as a potentially ubiquitous weakening mechanism, compatible with earthquake data over a very wide range of magnitudes [*Rice*, 2006; *Viesca and Garagash*, 2015]. Thermal pressurization is a mechanism by which faults weaken due to an increase in pore fluid pressure on the fault plane driven by frictional heating. In a purely empirical approach, *Nielsen et al.* [2016] have shown that the fracture energy derived from laboratory friction experiments, almost regardless of the experimental conditions, is in fact consistent with that of earthquakes. These experimental results highlight the potential nonuniqueness of the weakening mechanisms responsible for the scaling of G with slip: indeed, most of the experimental data used by *Nielsen et al.* [2016] were obtained on dry rocks, in a setup that essentially precludes the efficiency of thermal pressurization.

Overall, a key question is to determine what features of weakening mechanisms are essential to reproduce the scaling of G derived from seismological or experimental data, and whether weakening mechanisms other than thermal pressurization could also be viable candidates to explain the fracture energy of earthquakes.

Here we tackle this issue by exploring in detail the fracture energy associated with weakening by flash heating, which is a theoretically and experimentally documented weakening mechanism occurring at the onset of seismic slip [e.g., *Rice*, 1999, 2006; *Beeler et al.*, 2008; *Goldsby and Tullis*, 2011; *Passelègue et al.*, 2016; *Brantut et al.*, 2016]. We first present an updated flash heating model, which includes progressive weakening due to bulk frictional heating, and then compute the associated fracture energy under either imposed slip rate or within an elastodynamic crack model. We then discuss the resulting scaling of G with slip and compare it to experimental and earthquake data. Finally, we extract several general conclusions about how fracture energy should scale with slip for ruptures driven by thermal weakening processes.

2. Flash Heating Model

2.1. Governing Equations

The constitutive law governing frictional weakening by flash heating has been derived in detail by *Rice* [2006] and *Beeler et al.* [2008]. Here we develop a model for flash heating that is modified from the original formulation: following the steps initially outlined by *Rempel* [2006], and further developed by *Brantut and Platt* [2017] [see also *Proctor et al.*, 2014; *Yao et al.*, 2015], we include here the dependence of flash heating on the fault bulk temperature and extend the flash heating model to gouge. We first recall the general form of the shear strength evolution governed by flash heating [*Rice*, 1999, 2006; *Beeler et al.*, 2008]:

$$\tau = \tau_0 \frac{V_w(T)}{V}, \tag{1}$$

where τ is the strength, τ_0 is the initial frictional strength of the fault, V_w is a critical weakening slip rate (temperature-dependent), and V is the slip rate. Equation (1) is valid only for $V \geq V_w$, and τ is assumed to remain constant and equal to τ_0 at lower slip rates [*Rice*, 2006; *Beeler et al.*, 2008]. Here we do not include any "residual" strength level and assume that the strength at high slip rate approaches zero.

The weakening slip rate is given by [*Rice*, 2006]:

$$V_w(T) = \frac{\pi\alpha}{D}\left(\frac{\rho c(T_w - T)}{\tau_c}\right)^2, \tag{2}$$

where α is the thermal diffusivity of the fault rock, ρc is its heat capacity, D is the asperity contact diameter, τ_c is the asperity contact shear strength, and T_w is the critical weakening temperature. Equation (2) states that the weakening temperature is a function of the ambient temperature T, i.e., the background temperature of asperities before they start sliding.

The evolution of the shear strength of the fault is therefore given by the evolution of both the slip rate V and fault zone temperature T. The latter is a bulk average over many particles and asperities and is governed by the heat equation:

$$\frac{\partial T}{\partial t} = \alpha\frac{\partial^2 T}{\partial y^2} + \frac{\tau\dot{\gamma}}{\rho c}, \tag{3}$$

where y is the spatial coordinate normal to the fault surface, and $\dot{\gamma}$ is the distributed shear strain rate in the fault gouge. For a Gaussian strain rate distribution across the fault, equation (3) has the following solution for temperature evolution at $y = 0$ [*Carslaw and Jaeger*, 1959]:

$$T(t, y = 0) = T_0 + \frac{1}{\rho c}\int_0^t \frac{\tau(t')V(t')}{\sqrt{2\pi(w^2 + 2\alpha(t - t'))}}\mathrm{d}t', \tag{4}$$

where w is a measure of the shear zone thickness. The assumption of a Gaussian strain rate profile with constant w is a conservative one, since strain could further localize inside the gouge due to thermal weakening. Therefore, the temperature rise and resulting weakening are likely lower bound estimates. Using the expression (1) for shear stress, we obtain an expression for temperature that does not include any direct dependence on slip rate:

$$T(t, y = 0) = T_0 + \frac{\tau_0}{\rho c}\int_0^t \frac{V_w[T(t')]}{\sqrt{2\pi(w^2 + 2\alpha(t - t'))}}\mathrm{d}t'. \tag{5}$$

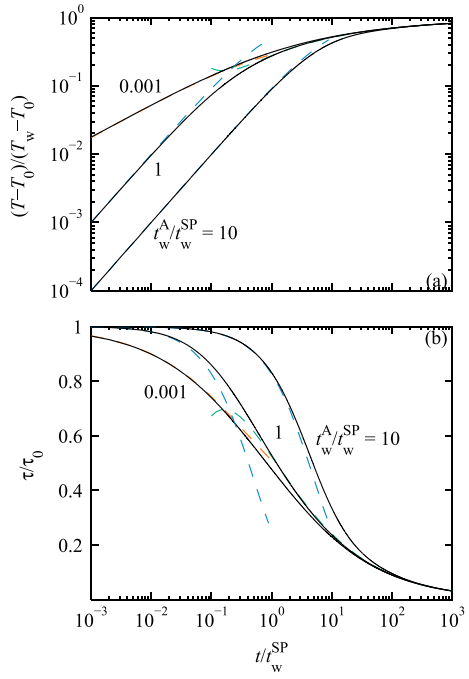

Figure 1. Evolution of (a) temperature and (b) strength with time during flash heating for a range of time scale ratios t_w^A/t_w^{SP}. The evolution of temperature (Figure 1a) is independent from the slip rate history. In the computation of strength we assumed $V = V_{w0}$. The black curves correspond to the full numerical solution for each ratio of time scales. The dashed blue lines correspond to the asymptotic solutions in the adiabatic regime, the dashed green lines are the asymptotic solutions for the slip-on-a-plane regime in the large time limit, and the dashed orange lines are the asymptotic solution for the slip-on-a-plane regime in the small time limit.

In our assumption of distributed strain rate over a finite thickness (and not bare surface contact), we implicitly extend the flash heating model to an ensemble of frictional contacts distributed over the fault thickness. This generalization has been developed by *Rempel* [2006] and *Brantut and Platt* [2017], who showed that the model would hold provided that V_w is modified by a factor proportional to the number of contacts within the fault thickness.

2.2. Solutions

In order to estimate the evolution of shear stress, and therefore of fracture energy, as a function of cumulated slip, one needs to solve equation (5). Three informative end-member solutions can be found analytically.

At early times, while the fault effective thickness $w\sqrt{2\pi}$ remains large compared to the thermal boundary layer width $\sqrt{\alpha t}$, heating is mostly adiabatic and equation (5) simplifies to

$$T - T_0 \approx \frac{\tau_0}{\rho c w\sqrt{2\pi}} \int_0^t V_w[T(t'))]\mathrm{d}t'. \qquad (6)$$

Combining with expression (2) for the weakening velocity, we obtain the following solution for temperature:

$$T(t) = T_0 + (T_w - T_0)\frac{t}{t + t_w^A}, \qquad (7)$$

where

$$t_w^A = \frac{\rho c(T_w - T_0)}{\tau_0}\frac{\sqrt{2\pi}w}{V_{w0}} \qquad (8)$$

with $V_{w0} = V_w(T_0)$. The time t_w^A corresponds to the time required to heat a layer of thickness $\sqrt{2\pi}w$ from $T = T_0$ up to the weakening temperature T_w. Equation (7) depends only on time and is not affected by the slip rate history on the fault.

At large times, when the thermal boundary layer becomes much wider than the shear zone thickness, shear heating is essentially concentrated on an infinitely narrow width, which acts as a line source. Under those conditions, equation (5) simplifies to

$$T - T_0 = \frac{\tau_0}{\rho c}\int_0^t \frac{V_w[T(t')]}{\sqrt{4\pi\alpha(t - t')}}\mathrm{d}t'. \qquad (9)$$

A natural characteristic time in this regime is the following:

$$t_w^{SP} = \alpha\left(\frac{\rho c(T_w - T_0)}{\tau_0 V_{w0}}\right)^2, \qquad (10)$$

which corresponds to the diffusion timescale that balances the nominal heat flux and the dissipation rate on the fault plane. A useful asymptotic solution, valid for $t \gg t_w^{SP}$, is given by (see supporting information section S1)

$$T(t) \approx T_0 + (T_w - T_0)\sqrt{2}\left(\pi t/t_w^{SP}\right)^{-1/4}. \qquad (11)$$

If we want to insist that the whole flash heating process occurs in the slip-on-a-plane limit, which is relevant for instance for bare rock frictional surfaces or when the two time scales t_w^A and t_w^{SP} are very different, we can also

determine a simple asymptotic form for $T(t)$ in the small time limit. For $t_w^A \ll t \ll t_w^{SP}$, we find (see supporting information section S1) that the temperature is well approximated by

$$T(t) \approx T_0 + (1/2)(T_w - T_0)\left(1 - \exp\left(t/t_w^{SP}\right)\operatorname{erfc}\left(\sqrt{t/t_w^{SP}}\right)\right). \quad (12)$$

Overall, for shear over a finite thickness, we observe that the temperature, and hence the strength evolution, is controlled by only two characteristic time scales, and therefore by only one-nondimensional parameter, namely, t_w^A/t_w^{SP}. This ratio of time scales controls the dominant thermal regime of the fault zone.

A set of numerical solutions of the general problem, computed using the spectral in space, finite-difference in time method given by *Noda and Lapusta* [2010], are shown in Figure 1a for a range of ratios t_w^A/t_w^{SP}, along with the asymptotic solutions derived above (see supporting information section S1 for second-order corrections to those). The corresponding evolution of strength, computed using (1) and $V = V_{w0}$, is given in Figure 1b. We observe a gradual decrease in strength over time, due to the reduction in $V_w(T)$ induced by the macroscopic heating of the fault.

3. Fracture Energy

Based on our strength computations, we can now make predictions for the fracture energy associated with flash heating. Here we use the generalized definition of G given by *Abercrombie and Rice* [2005]:

$$G(\delta) = \int_0^{\delta} \left(\tau[\delta'] - \tau[\delta]\right) \mathrm{d}\delta', \quad (13)$$

where δ is the slip. Since the strength depends directly on the slip rate history, we also expect the fracture energy to do so. In the following, we analyze how G scales with slip using two models for slip rate evolution, one with constant slip rate, and one derived from elastodynamics.

3.1. Analysis Using Constant Slip Rate

In a first approximation, we use a simple assumption of constant slip rate to compute G. In this case, analytical formulae can be derived for $G(\delta)$ in the three asymptotic cases outlined in the previous section. In the adiabatic regime, a direct computation of (13) using $\delta = Vt$ yields as follows:

$$G(\delta) = \rho c (T_w - T_0) w \sqrt{2\pi}\left(\frac{\delta}{Vt_w^A + \delta}\right)^2 \quad \text{(adiabatic)}. \quad (14)$$

In the slip-on-a-plane approximation, in the small slip limit (i.e., $Vt_w^A \ll \delta \ll Vt_w^{SP}$), an approximate form for the fracture energy is (see supporting information section S2)

$$G(\delta) \approx \tau_0 \delta_w^{SP} \times \frac{2}{3\sqrt{\pi}}\left(\frac{\delta}{\delta_w^{SP}}\right)^{3/2} \quad \text{(slip on a plane, small slip)}, \quad (15)$$

where $\delta_w^{SP} = V_{w0} t_w^{SP}$. Finally, a slip-on-a-plane, large slip approximation is given by (see supporting information section S2):

$$G(\delta) \approx \tau_0 \delta_w^{SP} \times \frac{2}{\sqrt{\pi}}\left(\frac{\delta}{\delta_w^{SP}}\right)^{1/2} \quad \text{(slip on a plane, large slip)}, \quad (16)$$

which is valid for $\delta \gg Vt_w^{SP}$. A second-order correction to the asymptotic behavior for G in the large-slip limit is discussed in supporting information section S2.

The results for $G(\delta)$ in the general case (computed numerically) and the approximate analytical solutions are shown in Figure 2. Essentially, we find that there is a switch from $G \propto \delta^2$ at small slip to $G \propto \sqrt{\delta}$ at large slip; if the two time scales t_w^A and t_w^{SP} are separated, an intermediate regime arises where $G \propto \delta^{3/2}$. This behavior is completely analogous to the scaling given by *Rice* [2006] for weakening by thermal pressurization.

The reason for the similarity between flash heating and thermal pressurization in this context is the fact that at small slip, both mechanisms are essentially similar to linear slip weakening; whereas at large slip, both mechanisms are dominated by a thermal weakening mechanisms controlled by a thermal (and/or hydraulic) diffusive boundary layer.

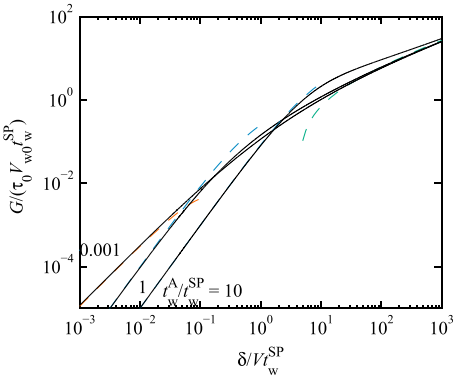

Figure 2. Evolution of fracture energy with slip during flash heating. This evolution is computed using a constant imposed slip rate. The black curves correspond to the full numerical solution for the given ratio of time scales t_w^A/t_w^{SP}. The dashed blue lines correspond to the asymptotic solution in the adiabatic regime, the dashed green line is the asymptotic solution for the slip-on-a-plane regime for large time, and the dashed orange line is the asymptotic solution for the slip-on-a-plane regime for small time.

3.2. Analysis Using a Dynamic Crack Model

The kinematic approach outlined above gives initial insight into the scaling of fracture energy with slip. However, using a constant slip rate is a simplification, inconsistent with the mechanics of rupture propagation in which slip rate evolves in concert with strength behind the rupture tip.

For a semi-infinite shear crack propagating at constant speed, the elastodynamic equilibrium requires that

$$\tau(x) = \frac{\mu^*}{2\pi V_r} \int_0^\infty \frac{V(s)}{s-x} \mathrm{d}s, \tag{17}$$

where x is the position from the rupture tip, V_r is the rupture speed and μ^* is an elastic shear modulus which depends on the mode of rupture and on the rupture speed [*Rice*, 1980]. The elastodynamic stress (17) has to be consistent with the strength on the fault given by the flash heating process (equation (1)). Therefore, the slip rate, stress, and temperature histories are coupled and have to be determined simultaneously.

Far from the crack tip, for large slip, an asymptotic analysis of the coupled system (17), (1), and (9) (see supporting information section S2) leads to the following approximation for the fracture energy:

$$G(\delta) \approx \tau_0 \delta_w^{SP} \left(\frac{\mu^* V_{w0}}{3\pi\tau_0 V_r} \right)^{1/3} \left(\frac{\delta}{\delta_w^{SP}} \right)^{2/3}. \tag{18}$$

Notably, G scaling with a 2/3 power law in slip was also found by *Viesca and Garagash* [2015] for dynamic ruptures driven by thermal pressurization.

4. Comparison With Laboratory and Earthquake Data

The theoretical results outlined in the previous section can be compared to laboratory data obtained at high constant (imposed) slip rate. Figure 3 shows the fracture energy compilation of *Nielsen et al.* [2016] as a function slip, plotted together with the theoretical predictions for flash heating using a realistic set of parameter values [*Brantut and Platt*, 2017]: constant slip rate V = 1 m/s, critical time t_w^{SP} = 0.1 s, critical slip rate V_{w0} = 0.2 m/s, and nominal stress τ_0 = 20 MPa. The flash heating model reproduces the shift in trend, modeled here as a transition between $\delta^{3/2}$ at small slip and $\delta^{1/2}$ at large slip.

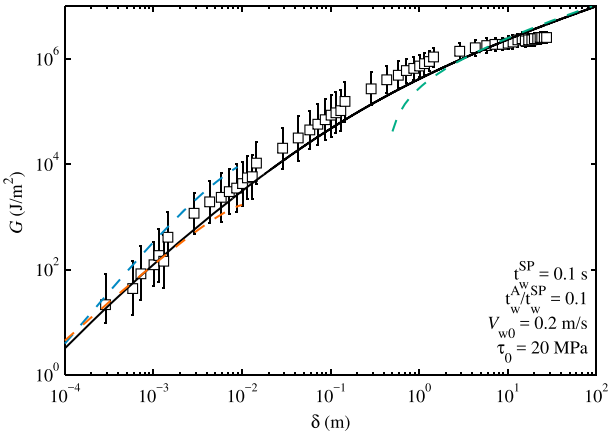

Figure 3. Comparison of laboratory-derived fracture energy from high-speed friction experiments [*Nielsen et al.*, 2016] (squares) and theoretical predictions for flash heating. The general numerical solution is given by the solid black line, the large slip asymptote is the green dashed line, the small slip (adiabatic) asymptote is the blue dashed line, and the small slip (slip-on-a-plane) asymptote is the orange dashed line. Parameter values are listed in the graph.

The theoretical results for the dynamic crack-tip problem can be used to see whether we can also explain earthquake fracture energy data with flash heating only. This is attempted in Figure 4, which shows the G versus δ data compiled by *Viesca and Garagash* [2015] together with the large slip asymptote obtained from the dynamic

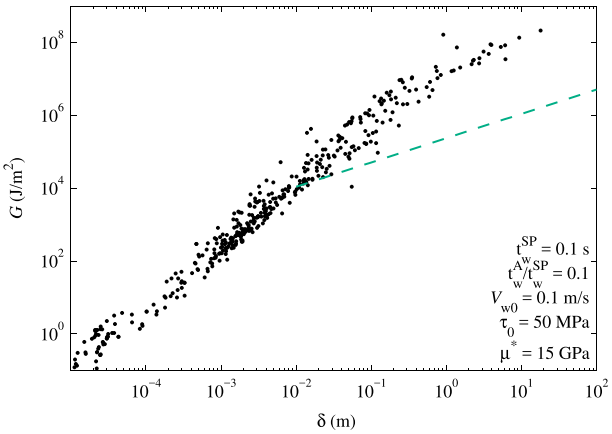

Figure 4. Comparison of earthquake fracture energy estimates (taken from the compilation of *Viesca and Garagash* [2015]) and the semi-infinite crack model driven by flash heating only (large slip asymptote shown as the green dashed line). Parameter values are reported in the graph.

steady state crack analysis. We used a rupture speed V_r equal to around 90% of the shear wave speed, so that the elastodynamic shear modulus μ^* is reduced by approximately a factor 2 compared to its static value.

Even though the set of parameters used in the simulation are similar to that used to fit the laboratory data, the fracture energy predicted by the model remains much smaller than for earthquakes over a significant range of slip ($\delta > 10^{-2}$ m). Beyond 10 mm slip, the fracture energy from flash heating is much smaller than for earthquakes, implying that other dissipation processes dominate (e.g., thermal pressurization). This is consistent with previous estimates for the relative contribution of flash heating versus thermal pressurization [*Brantut and Rice*, 2011]. In Figure 4 we used a value for V_{w0} consistent with bare rock surfaces; in gouge, V_{w0} should be divided by a factor commensurate with the number of contacts within the gouge thickness. This modification would increase the value of fracture energy but has little quantitative impact due to the weak sensitivity of G to V_{w0} (power $-1/3$). Furthermore, the correction of V_{w0} for gouge at large slip is likely small because of the potential strain localization occurring during the early stages of slip.

At small slip distances, the earthquake data are consistent with a scaling of G with δ^2, as for instance produced by a linear slip-weakening friction law (as long as the constant residual friction is not reached) or by thermal pressurization of pore fluids. Note that slip weakening is not necessarily incompatible with the physics of flash heating, since there must be a critical slip distance beyond which asperities start to weaken at high speed [e.g., *Noda et al.*, 2009; *Brantut and Rice*, 2011; *Viesca and Garagash*, 2015]. Here we did not include any slip-weakening process in our flash heating model in order to explore the properties of the thermal weakening process alone. It appears that the involvement of an element of slip weakening at small slip distances within the flash heating framework is necessary to produce a more realistic scaling of fracture energy with slip.

Despite the similarity in the scaling of G with slip between thermal pressurization and flash heating at large slip ($G \propto \delta^{2/3}$), any quantitative estimate using realistic parameter values reveals that flash heating has a negligible contribution in G.

5. Discussion and Conclusion

Laboratory data are explained quantitatively well by the flash heating model, but not earthquake data, especially for slip distances larger than a few millimeters. By contrast, *Viesca and Garagash* [2015] have shown that thermal pressurization is able explain earthquake data over 9 orders of magnitude in slip. This difference is due mostly to the low heat diffusivity of rocks, which make critical weakening times and distances for flash heating very short compared to those linked with thermal pressurization (see supporting information section S3). Indeed, the characteristic slip distance associated with thermal pressurization is governed by the hydraulic diffusivity of fault rocks, which is widely variable and typically orders of magnitude larger than their thermal diffusivity. In addition, the large slip rates arising in the elastodynamic crack model tend to induce a faster strength reduction than in constant slip rate cases, therefore producing overall lower fracture energies.

Despite the quantitative discrepancies between flash heating and thermal pressurization, for both processes the fracture energy at large slip scales with $\delta^{1/2}$ at constant slip rate and with $\delta^{2/3}$ for propagating ruptures. This similarity is not coincidental; in fact, *any* thermal weakening process for which temperature remains bounded at large times would produce similar scalings of G with slip. Indeed, the large slip asymptote is obtained by observing that (1) $V(x)$ and $\tau(x)$ both decrease with same power x^λ far from the crack tip (equation (17), see *Viesca and Garagash* [2015] and supporting information) and (2) the integral

in (4) approaches a constant, finite temperature for sufficiently large times. These requirements imply that $\lambda = -1/4$, from which $G \propto \delta^{2/3}$ is deduced.

By contrast, the apparent stronger scaling of G with δ^2 at small slip merely reflects a linear slip-weakening process. Thermal pressurization under adiabatic, undrained conditions is a likely possibility but may not be the only one. For instance, a regularized flash heating process including an intrinsic critical slip distance for asperities to weaken [*Noda et al.*, 2009] would also be a possibility.

From a phenomenological point of view, brittle fracture of intact rocks is also characterized by a slip-weakening process [e.g., *Ohnaka*, 2003], and so does rate-and-state friction at moderate slip rates (i.e., in the absence of healing or state recovery). Any of these phenomena is compatible with seismological estimates of $G(\delta)$ for small slip (typically $\delta \lesssim 1$ cm).

In summary, the most general conclusion that can be drawn from the comparison of friction models and seismological constraints of fracture energy is that seismic slip occurs by a succession or combination of physical processes which (1) initially resemble linear slip weakening and (2) progressively become dominated by diffusion across the fault. In other words, the progressive change in scaling of G versus slip with increasing slip imply that shear work dissipation occurs more and more outside the fault, either due to thermal or hydraulic diffusion (as in flash heating or thermal pressurization) or alternatively by off-fault damage (as explained by *Andrews* [1976, 2005] and *Nielsen et al.* [2016]).

The theoretical developments presented here show that great care is required when comparing friction models (empirical or physics based) to earthquake data: except for the purely slip-dependent friction laws, boundary conditions in terms of slip rate history generally have an impact on the strength evolution and on the resulting fracture energy. Dynamic steady state rupture models [e.g., *Garagash*, 2012; *Viesca and Garagash*, 2015] provide a useful tool to circumvent the shortcomings of assuming a priori slip rate histories, without having to resort to computationally intensive numerical elastodynamic simulations.

Acknowledgments
This work was initiated following discussions with John D. Platt, whom both authors would like to gratefully acknowledge. N.B. received support from the UK Natural Environment Research Council through grant NE/K009656/1. R.C.V. is grateful for support from NSF grant EAR-1344993 and from the Southern California Earthquake Center (SCEC). SCEC is funded by NSF Cooperative Agreement EAR-1033462 and USGS Cooperative Agreement G12AC20038. The SCEC contribution number for this paper is 7291. The analytical formulae and numerical methods described in the main text and supporting information are sufficient to reproduce all the results presented in the paper.

References

Abercrombie, R. E., and J. R. Rice (2005), Can observations of earthquake scaling constrain slip weakening?, *Geophys. J. Int.*, *162*, 406–424.
Andrews, D. J. (1976), Rupture propagation with finite stress in antiplane strain, *J. Geophys. Res.*, *81*(20), 3575–3582.
Andrews, D. J. (2005), Rupture dynamics with energy loss outside the slip zone, *J. Geophys. Res.*, *110*, B01307, doi:10.1029/2004JB003191.
Beeler, N. M., T. E. Tullis, and D. L. Goldsby (2008), Constitutive relationships and physical basis of fault strength due to flash heating, *J. Geophys. Res.*, *113*, B01401, doi:10.1029/2007JB004988.
Brantut, N., and J. D. Platt (2017), Dynamic weakening and the depth dependence of earthquake faulting, in *Fault Zone Dynamic Processes: Evolution of Fault Properties During Seismic Rupture, Geophys. Monogr. Ser.*, vol. 227, edited by M. Y. Thomas, T. M. Mitchell, and H. S. Bhat, pp. 171–194, AGU, Washington, D. C.
Brantut, N., and J. R. Rice (2011), How pore fluid pressurization influences crack tip processes during dynamic rupture, *Geophys. Res. Lett.*, *38*, L24314, doi:10.1029/2011GL050044.
Brantut, N., F. X. Passelègue, D. Deldicque, J.-N. Rouzaud, and A. Schubnel (2016), Dynamic weakening and amorphization in serpentinite during laboratory earthquakes, *Geology*, *44*(8), 607–610, doi:10.1130/G37932.1.
Carslaw, H. S., and J. C. Jaeger (1959), *Conduction of Heat In Solids*, 2nd ed., Oxford Univ. Press, New York.
Garagash, D. I. (2012), Seismic and aseismic slip pulses driven by thermal pressurization of pore fluid, *J. Geophys. Res.*, *117*, B04314, doi:10.1029/2011JB008889.
Goldsby, D. L., and T. E. Tullis (2011), Flash heating leads to low frictional strength of crustal rocks at earthquake slip rates, *Science*, *334*, 216–218.
Guatteri, M., and P. Spudich (2000), What can strong-motion data tell us about slip-weakening fault-friction laws?, *Bull. Seismol. Soc. Am.*, *90*(1), 98–116.
Kanamori, H., and T. H. Heaton (2000), Microscopic and macroscopic physics of earthquakes, in *Geocomplexity and the Physics of Earthquakes, Geophys. Monogr. Ser.*, vol. 120, edited by J. B. Rundle, D. L. Turcotte, and W. Klein, pp. 147–163, AGU, Washington, D. C.
Nielsen, S., E. Spagnuolo, S. A. F. Smith, M. Violay, G. Di Toro, and A. Bistacchi (2016), Scaling in natural and laboratory earthquakes, *Geophys. Res. Lett.*, *43*, 1504–1510, doi:10.1002/2015GL067490.
Noda, H., and N. Lapusta (2010), Three-dimensional earthquake sequence simulations with evolving temperature and pore pressure due to shear heating: Effect of heterogeneous hydraulic diffusivity, *J. Geophys. Res.*, *115*, B12314, doi:10.1029/2010JB007780.
Noda, H., E. M. Dunham, and J. R. Rice (2009), Earthquake ruptures with thermal weakening and the operation of major faults at low overall stress levels, *J. Geophys. Res.*, *114*, B07302, doi:10.1029/2008JB006143.
Ohnaka, M. (2003), A constitutive scaling law and a unified comprehension for frictional slip failure, shear fracture of intact rock, and earthquake rupture, *J. Geophys. Res.*, *108*(B2), 2080, doi:10.1029/2000JB000123.
Passelègue, F. X., A. Schubnel, S. Nielsen, H. S. Bhat, D. Deldicque, and R. Madariaga (2016), Dynamic rupture processes inferred from laboratory microearthquakes, *J. Geophys. Res. Solid Earth*, *121*, 4343–4365, doi:10.1002/2015JB012694.
Proctor, B. P., T. M. Mitchell, G. Hirth, D. Goldsby, F. Zorzi, J. D. Platt, and G. Di Toro (2014), Dynamic weakening of serpentinite gouge and bare-surfaces at seismic slip rates, *J. Geophys. Res. Solid Earth*, *119*, 8107–8131, doi:10.1002/2014JB011057.
Rempel, A. W. (2006), The effects of flash-weakening and damage on the evolution of fault strength and temperature, in *Earthquakes: Radiated Energy and the Physics of Faulting, Geophys. Monogr. Ser.*, vol. 170, edited by R. Abercrombie et al., pp. 263–270, AGU, Washington, D. C.

Rice, J. R. (1980), The mechanics of earthquake rupture, in *Physics of the Earth's Interior, Proc. Int. School of Phys. E. Fermi*, edited by A. M. Dziewonski and E. Boschi, pp. 555–649, Italian Phys. Soc./North Holland, Amsterdam.

Rice, J. R. (1999), Flash heating at asperity contacts and rate-dependent friction, *Eos Trans. AGU*, *80*(46), Fall Meet. Suppl., F6811.

Rice, J. R. (2006), Heating and weakening of faults during earthquake slip, *J. Geophys. Res.*, *111*, B05311, doi:10.1029/2005JB004006.

Viesca, R. C., and D. I. Garagash (2015), Ubiquitous weakening of faults due to thermal pressurization, *Nat. Geosci.*, *8*, 875–879, doi:10.1038/ngeo2554.

Yao, L., S. Ma, J. D. Platt, A. Niemeijer, and T. Shimamoto (2015), The crucial role of temperature in high-velocity weakening of faults: Experiments on gouge using host blocks of different thermal conductivities, *Geology*, *44*, 63–66, doi:10.1130/G37310.1.